

This discussion paper is/has been under review for the journal *Atmospheric Chemistry and Physics (ACP)*. Please refer to the corresponding final paper in *ACP* if available.

# Atmospheric OH reactivities in the Pearl River Delta – China in summer 2006: measurement and model results

S. Lou<sup>1,2</sup>, F. Holland<sup>2</sup>, F. Rohrer<sup>2</sup>, K. Lu<sup>3,2</sup>, B. Bohn<sup>2</sup>, T. Brauers<sup>2</sup>, C. C. Chang<sup>6</sup>, H. Fuchs<sup>2</sup>, R. Häseler<sup>2</sup>, K. Kita<sup>4</sup>, Y. Kondo<sup>5</sup>, X. Li<sup>3,2</sup>, M. Shao<sup>3</sup>, L. Zeng<sup>3</sup>, A. Wahner<sup>2</sup>, Y. Zhang<sup>3</sup>, W. Wang<sup>1</sup>, and A. Hofzumahaus<sup>2</sup>

<sup>1</sup>School of Environmental Science and Technology, Shanghai Jiatong Univ., Shanghai, China

<sup>2</sup>Institut für Chemie und Dynamik der Geosphäre 2: Troposphäre, Forschungszentrum Jülich, Jülich, Germany

<sup>3</sup>College of Environmental Sciences and Engineering, Peking Univ., Beijing, China

<sup>4</sup>Faculty of Science, Ibaraki Univ., Ibaraki, Japan

<sup>5</sup>Research Center for Advanced Science and Technology, Univ. of Tokyo, Tokyo, Japan

<sup>6</sup>Research Center for Environmental Changes (RCEC), Academic Sinica, Taipei, China

Received: 4 August 2009 – Accepted: 7 August 2009 – Published: 12 August 2009

Correspondence to: A. Hofzumahaus (a.hofzumahaus@fz-juelich.de) and W. Wang (whwang@sjtu.edu.cn)

Published by Copernicus Publications on behalf of the European Geosciences Union.

OH reactivity  
measurement

S. Lou et al.

Title Page

Abstract

Introduction

Conclusions

References

Tables

Figures

◀

▶

◀

▶

Back

Close

Full Screen / Esc

Printer-friendly Version

Interactive Discussion



## Abstract

Total atmospheric OH reactivities ( $k_{\text{OH}}$ ) have been measured as reciprocal OH lifetimes by a newly developed instrument at a rural site in the densely populated Pearl River Delta (PRD) in Southern China in summer 2006. The deployed technique, LP-LIF, uses laser flash photolysis (LP) for artificial OH generation and laser-induced fluorescence (LIF) to measure the time-dependent OH decay in samples of ambient air. The reactivities observed at PRD covered a range from  $10 \text{ s}^{-1}$  to  $120 \text{ s}^{-1}$ , indicating a large load of chemical reactants. On average,  $k_{\text{OH}}$  exhibited a pronounced diurnal profile with a mean maximum value of  $50 \text{ s}^{-1}$  at daybreak and a mean minimum value of  $20 \text{ s}^{-1}$  at noon. The reactivity was dominated by anthropogenic pollutants (e.g., CO,  $\text{NO}_x$ , light alkenes and aromatic hydrocarbons) at night, while it was strongly influenced by local, biogenic emissions of isoprene at day. The comparison of reactivities calculated from measured trace gases with measured  $k_{\text{OH}}$  reveals a missing reactivity of about a factor of 2 at day and night. Box model calculations initialized by measured parameters reproduce the observed OH reactivity well and suggest that the missing reactivity is contributed by unmeasured, secondary chemistry products (mainly aldehydes and ketones) that were photochemically formed by hydrocarbon oxidation. Overall,  $k_{\text{OH}}$  was dominated by organic compounds, which had a maximum contribution of 85% in the afternoon. The paper demonstrates the usefulness of direct reactivity measurements and emphasizes the need for direct measurements of oxygenated organic compounds in atmospheric chemistry studies.

## 1 Introduction

The hydroxyl radical (OH) is the primary oxidant in the troposphere. It reacts with most atmospheric trace gases and, thereby, controls their rate of removal from the atmosphere (Ehhalt, 1999). In many cases, oxidation of primary pollutants by OH leads to formation of hydroperoxy ( $\text{HO}_2$ ) and organic peroxy radicals ( $\text{RO}_2$ , R=organic

## OH reactivity measurement

S. Lou et al.

Title Page

Abstract

Introduction

Conclusions

References

Tables

Figures

◀

▶

◀

▶

Back

Close

Full Screen / Esc

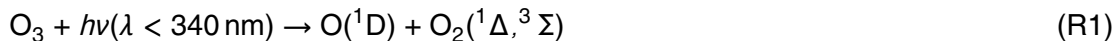
Printer-friendly Version

Interactive Discussion



group) which are important intermediates in the photochemical formation of ozone and organic aerosols. A good understanding of tropospheric OH and its related chemistry is therefore indispensable for reliable prediction of the atmospheric self-cleansing and the formation of secondary atmospheric pollutants (Brasseur et al., 2003).

Tropospheric OH is produced primarily by a few relatively well-known processes, of which the UV photolysis of ozone is the most important one (Matsumi et al., 2002).

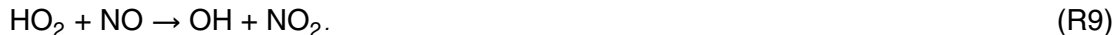


- 5 Other relevant processes include the photolysis of nitrous acid and ozonolysis of alkenes.

OH exhibits a high reactivity to many atmospheric trace components such as carbon monoxide (CO), nitrogen oxides (NO, NO<sub>2</sub>) and volatile organic compounds (VOCs). OH reactions with CO and hydrocarbons (RH) produce peroxy radicals (HO<sub>2</sub>, RO<sub>2</sub>).



Subsequent reactions of RO<sub>2</sub> and HO<sub>2</sub> with NO recycle OH.



Here, RO represents short-lived alkoxy radicals and R'O indicates carbonyl compounds (aldehydes, ketones).

OH loss can also occur by recombination reactions, which ultimately remove radicals from the atmosphere. In this class of reactions, association between OH and NO<sub>2</sub> is

**OH reactivity  
measurement**

S. Lou et al.

Title Page

Abstract

Introduction

Conclusions

References

Tables

Figures

◀

▶

◀

▶

Back

Close

Full Screen / Esc

Printer-friendly Version

Interactive Discussion



the most important example.



Atmospheric OH is short-lived (<1 s) reaching a steady state of production and loss within a few seconds.

$$\frac{d[\text{OH}]}{dt} = P_{\text{OH}} - k_{\text{OH}}[\text{OH}] \simeq 0 \quad (1)$$

In this equation,  $P_{\text{OH}}$  is the total production rate of OH from primary production (e.g., R2) and radical recycling reactions (e.g., R9), while  $k_{\text{OH}}$  represents the pseudo first-order rate coefficient of OH in ambient air.  $k_{\text{OH}}$  is also called total OH reactivity and is equivalent to the reciprocal atmospheric OH lifetime,  $\tau_{\text{OH}}^{-1}$ .

$$k_{\text{OH}} = \sum k_{\text{OH}+\text{X}_i}[\text{X}_i] = \tau_{\text{OH}}^{-1} \quad (2)$$

Here,  $[\text{X}_i]$  represents the concentration of a reactive component (CO,  $\text{NO}_x$ , VOCs etc.) in ambient air,  $k_{\text{OH}+\text{X}_i}$  denotes the corresponding bimolecular reaction rate constant and  $k_{\text{OH}+\text{X}_i}[\text{X}_i]$  the reactivity of  $\text{X}_i$ .

A major uncertainty in atmospheric chemistry results from incomplete knowledge of number and abundance of reactive components being present in the atmosphere. Besides well-known pollutants like CO and  $\text{NO}_x$ , a large number of probably more than  $10^5$  different VOCs exists in the troposphere (Goldstein and Galbally, 2007), but less than one hundred VOCs are measured routinely in field campaigns. The measured VOC species are thought to represent the major organic reactivity. Recent field experiments, however, demonstrate that a considerable fraction of organic components missed by current measurement techniques may have significant influence on atmospheric photochemistry (Lewis et al., 2000; Di Carlo et al., 2004; Sadanaga et al., 2005; Holzinger et al., 2005; Goldstein and Galbally, 2007; Heald et al., 2008; Mao et al., 2009). Thus, incomplete VOC measurements and unknown atmospheric components can introduce considerable uncertainty in model predictions, for example, of atmospheric OH (Pope et al., 1994; McKeen et al., 1997).

## OH reactivity measurement

S. Lou et al.

Title Page

Abstract

Introduction

Conclusions

References

Tables

Figures

◀

▶

◀

▶

Back

Close

Full Screen / Esc

Printer-friendly Version

Interactive Discussion



**OH reactivity  
measurement**

S. Lou et al.

Title Page

Abstract

Introduction

Conclusions

References

Tables

Figures

◀

▶

◀

▶

Back

Close

Full Screen / Esc

Printer-friendly Version

Interactive Discussion



An important approach to this problem was the development of perturbation techniques that introduce artificially generated OH into samples of ambient air and measure directly the total OH reactivity. Some field instruments measure  $k_{\text{OH}}$  as the inverse of the atmospheric OH lifetime, either in a reaction flow tube with a movable OH injector (Kovacs and Brune, 2001; Mao et al., 2009; Ingham et al., 2009) or by using a laser pump and probe technique (Calpini et al., 1999; Sadanaga et al., 2004b; Hofzumahaus et al., 2009). Another concept involves the comparative  $k_{\text{OH}}$  measurement in a flow cell against the known OH reactivity of an added organic reagent (Sinha et al., 2008). Using these various techniques,  $k_{\text{OH}}$  values have been observed between  $1 \text{ s}^{-1}$  in clean air and  $200 \text{ s}^{-1}$  in extremely polluted air in the atmospheric boundary layer (Table 1).

Measurements of  $k_{\text{OH}}$  provide valuable information and can be useful in atmospheric chemistry studies in different ways. First, experimental  $k_{\text{OH}}$  data provide the chemical reactivity that would be expected by calculation from individual trace gas measurements ( $k_{\text{OH}}^{\text{calc}}$ ), if all atmospheric OH reactants are completely measured. The ratio  $k_{\text{OH}}/k_{\text{OH}}^{\text{calc}}$  allows to quantify the amount of reactivity that remains unmeasured or unidentified in field experiments. Missing reactivity has been reported for different environments, including marine, rural and urban sites, with measured-to-calculated reactivity ratios as high as 3 (Table 1).

Second,  $k_{\text{OH}}$  data can be used to estimate the atmospheric VOC reactivity, if measured data of non-VOC compounds ( $Y_i = \text{CO}, \text{NO}_x$  etc.) are simultaneously available:

$$k_{\text{OH}}(\text{VOC}) \simeq k_{\text{OH}} - \sum k_{\text{OH}+Y_i}[Y_i] \quad (3)$$

Shirley et al. (2006) and Ren et al. (2005, 2006b) have used such  $k_{\text{OH}}(\text{VOC})$  data together with typical VOC speciation patterns as constraints for model predictions of OH, when direct VOC measurements were not completely available.

Third, OH reactivity measurements are useful to evaluate experimentally the chemical OH budget (Martinez et al., 2003; Ren et al., 2003b; Shirley et al., 2006; Hofzumahaus et al., 2009). Possible, unidentified OH production processes can be quantified by comparison of the experimental OH loss rate,  $k_{\text{OH}} \times [\text{OH}]$ , calculated from measured

OH and  $k_{\text{OH}}$ , with  $P_{\text{OH}}$  data derived from measured OH precursors. Such study was carried out by Hofzumahaus et al. (2009) for data from a field campaign in the Pearl River Delta (PRD) in China in summer 2006. By comparing the total OH loss and production rates, a significant missing OH source was discovered, which sustained high levels of OH in the order of  $10^7$  radicals per  $\text{cm}^3$  at conditions of low NO ( $<1$  ppb) and high OH reactivities ( $\sim 20 \text{ s}^{-1}$ ).

Lastly,  $k_{\text{OH}}$  data can be used to test the capability of photochemistry models to simulate atmospheric OH loss rates. This is part of the present paper where OH reactivities from the above mentioned PRD field campaign are presented. Observed reactivities are compared to  $k_{\text{OH}}^{\text{calc}}$  calculations from individual trace gas measurements and to simulated reactivities  $k_{\text{OH}}^{\text{model}}$  from a photochemical box model. The paper presents the chemical speciation of reactants contributing mostly to the OH loss rate at PRD and investigates, how well modelled, yet unmeasured secondary chemical products explain the missing reactivity observed during the campaign.

## 2 Field site and campaign

PRD is located in Southern China in Guangdong province and represents one of the major industrialized regions in Asia, with more than 20 million inhabitants. PRD includes the megacities of Hong Kong, Shenzhen and Guangzhou, and many fast-developing mid and small sized cities that are linked by a dense traffic network (Zhang et al., 2008b). Owing to the fast growing economy and urbanization, air pollution has greatly increased in this region during the last decade (Richter et al., 2005; Shao et al., 2006; Tie et al., 2006; Chan and Yao, 2008; Zhang et al., 2007, 2008b,a). Within the “Program of Regional Integrated Experiments of Air Quality over the Pearl River Delta” the photochemistry field campaign PRIDE-PRD2006 was conducted in summer 2006, aiming to investigate gas-phase chemistry and aerosol processes in a rural environment near Guangzhou city (Zhang et al., 2009, in preparation). Measurements were performed from 3 to 30 July 2006 at Backgarden (23.5° N, 113.03° E), a regional back-

### OH reactivity measurement

S. Lou et al.

Title Page

Abstract

Introduction

Conclusions

References

Tables

Figures

◀

▶

◀

▶

Back

Close

Full Screen / Esc

Printer-friendly Version

Interactive Discussion



**OH reactivity  
measurement**

S. Lou et al.

Title Page

Abstract

Introduction

Conclusions

References

Tables

Figures

◀

▶

◀

▶

Back

Close

Full Screen / Esc

Printer-friendly Version

Interactive Discussion



ground site about 60 km northwest of Guangzhou. Backgarden is located near a water reservoir and is surrounded by farmland (peanuts, Lichees, trees). It experienced little local emissions from traffic, but biomass burning was occasionally observed on nearby agricultural fields. Temperature and relative humidity were generally high, showing values of 28–36°C and 60–90% r.H., respectively, as is expected for a subtropical region during the rainy season. Extended rain fall occurred during two periods under the influence of typhoon Bilis (15–18 July) and Kaemi (26–29 July). At the field site, local wind speeds were generally low and had values mostly less than 2 m/s. Such low wind speeds are typical in the inland of PRD during summer season and favor accumulation of air pollution (Chan and Yao, 2008).

Measurement instruments were operated at Backgarden to characterize the local atmosphere with respect to its gas phase composition (Hua et al., 2008; Hofzumahaus et al., 2009) and aerosol abundance and properties (Li et al., 2008; Liu et al., 2008a; Garland et al., 2008; Rose et al., 2008; Xiao et al., 2009). Mixing ratios of VOCs, CO, SO<sub>2</sub>, O<sub>3</sub>, H<sub>2</sub>O<sub>2</sub>, NO<sub>x</sub> and photolysis frequencies were measured at 10 m above ground on top of a hotel building that was exclusively used by the measurement team. Additional measurements of radical concentrations of OH and HO<sub>2</sub>, atmospheric OH reactivities, mixing ratios of HONO and meteorological data were performed nearby at 7 m height on top of two stacked sea containers. Atmospheric chemical species considered in this work are listed in Tables 2 and 3.

### 3 Experimentals

#### 3.1 Measurements of $k_{OH}$

Total atmospheric OH reactivities were measured as inverse chemical OH lifetimes by a newly developed instrument, which is based on a pump-probe concept similar to the one explored by Calpini et al. (1999) and developed for field measurement by Sadanaga et al. (2004b). Laser flash photolysis (LP) of ozone is used to produce OH in

**OH reactivity  
measurement**

S. Lou et al.

Title Page

Abstract

Introduction

Conclusions

References

Tables

Figures

◀

▶

◀

▶

Back

Close

Full Screen / Esc

Printer-friendly Version

Interactive Discussion



a sample of ambient air and laser-induced fluorescence (LIF) is applied to monitor the time dependent OH decay. A short description of the LP-LIF instrument is given below, while technical details will be reported elsewhere (Lou et al., 2009, in preparation).

For measurement, ambient air is sampled through an 8 m long inlet-line (Silcosteel®, 8 mm i.D.) and is passed through a laminar flow tube at a rate of 20 litre/min at atmospheric pressure. In the PRD campaign, temperatures of the sampling line and flow tube were kept at 40°C, slightly above ambient temperature, to avoid possible condensation of water vapor in the instrument that was housed in an airconditioned field container. The flow tube has a total length of 80 cm and an internal diameter of 40 mm. A pulsed laser beam (266 nm, 10–20 mJ, FWHM 10 ns) from a frequency-quadrupled Nd-YAG laser (Big Sky, CFR200) is expanded to a diameter of 30 mm and is passed longitudinally through the centre of the flow tube, thereby generating OH radicals by flash photolysis of ozone (Reactions R1, R2). The OH radicals react subsequently with the trace gases in the carrier flow on a time scale of tens to hundreds of milliseconds. About 50 cm downstream of the tube inlet, part of the air flow (3 litre/min) is diverted through an inlet nozzle into a low pressure cell for OH detection by LIF. The detection cell is essentially of the same type as for ambient OH radical measurement (Holland et al., 2003). The probe laser radiation (308 nm) comes from a tunable, frequency-doubled 8.5 kHz pulsed dye laser (New Laser Generation, Tintura) which is shared between the OH reactivity instrument and the instrument for measurement of atmospheric HO<sub>x</sub> concentrations. With this setup, the time-dependent chemical OH decay is probed by LIF while the flowing air passes through the tube along the inlet of the detection cell. The OH fluorescence signal is collected in a time-resolved mode in a multichannel scaler (Becker and Hickl, PM400A) and is stored in an array of time bins of 1 ms width over a time period of 2 s. Decay curves are accumulated (signal-averaged) over successive photolysis pulses at a rate of 0.5 Hz to obtain a good signal-to-noise ratio. Examples of OH decay curves measured during the PRD field campaign 2006 are shown in Fig. 1. OH reactivities (reciprocal OH lifetimes) are obtained by non-linear least squares fits (CURVEFIT IDL-routine, Research Systems, Inc.) of the exponen-

**OH reactivity  
measurement**

S. Lou et al.

Title Page

Abstract

Introduction

Conclusions

References

Tables

Figures

◀

▶

◀

▶

Back

Close

Full Screen / Esc

Printer-friendly Version

Interactive Discussion



tial decay curves. The precision of the derived  $k_{\text{OH}}$  values is between 4–10% ( $1\sigma$ ). In clean synthetic air, zero decays resulting from OH wall loss can be observed. At PRD, the zero decays had rate coefficients of  $1.4 \pm 0.3 \text{ s}^{-1}$ , which were subtracted from the ambient air measurements. The integration time for the  $k_{\text{OH}}$  measurements was typically 1–3 min.

Ozone from an ozone generator was added to the gas samples when they contained less than 10 ppb  $\text{O}_3$ . This was the case during zero decay measurements and during air measurements at nighttime when ambient ozone dropped to low values. On these occasions, a controlled flow of 0.4 litre/min of synthetic air was ozonized and mixed into the main flow (20 litre/min), resulting in a mixing ratio of about 50 ppb  $\text{O}_3$  entering the flow tube. The marginal dilution (2%) of the main flow was corrected in the evaluation of the measured OH reactivities.

The accuracy of the instrument was tested before and after the campaign using air mixtures (e.g., CO in synthetic air) of known reactivities. The measurements were found to be linear for reactivities up to  $60 \text{ s}^{-1}$  and were accurate within 10% (Hofzumahaus et al., 2009). At  $k_{\text{OH}}$  larger than  $60 \text{ s}^{-1}$ , an increasing negative bias was noted in the measurement data, which was caused by the non-exponential curvature of the OH decay curves in the first 20 ms (Fig. 1). The deviations from the true reactivity were, for example,  $-11\%$  at  $80 \text{ s}^{-1}$  and  $-18\%$  at  $100 \text{ s}^{-1}$ . This non-linearity affects less than 2% of the data points measured at PRD and was corrected using a parametrization based on results of the test measurements (Lou et al., 2009).

Recycling of  $\text{HO}_2$  to OH (Reaction R9) can slow down the observed OH decay in the reactor, if the reaction rate of  $\text{HO}_2$  and NO approaches the OH decay rate (Kovacs et al., 2003). This is generally the case after most OH has initially reacted with CO and VOCs, provided that sufficient NO is available. As a result, the observed  $k_{\text{OH}}$  becomes systematically smaller than the true  $k_{\text{OH}}$ . The data correction for the NO dependent effect can be large in measurement systems that inject not only OH into the reactor, but also  $\text{HO}_2$ . This is the case in instruments that generate OH and  $\text{HO}_2$  as co-products by 185 nm photolysis of water vapor (Kovacs et al., 2003; Shirley et al., 2006; Sinha

et al., 2008; Ingham et al., 2009). For example, a correction factor of 1.4 at 5 ppb NO has been reported by Kovacs et al. (2003).

The LP-LIF technique is much less affected by NO since no significant HO<sub>2</sub> is initially generated (Sadanaga et al., 2004b). Thus, in the present work, the error caused by reaction R9 is mostly negligible, reaching at most 5% at 5 ppb NO at PRD conditions. At higher NO, biexponential behaviour of the OH decays became noticeable, which can be explained by radical recycling. In this case, a biexponential fit was applied to the measured OH decay curves. The faster of the two fitted decay rate coefficients was used as an estimator of the true  $k_{\text{OH}}$ . The validity of this approximation was confirmed by numerical simulations and laboratory experiments, demonstrating that the error of this approach is less than 10% for PRD conditions (Lou et al., 2009).

### 3.2 Trace gas measurements

OH concentrations were measured by LIF spectroscopy (Holland et al., 2003; Hofzumahaus et al., 2009). Ambient air was sampled by gas expansion into a low-pressure (3.5 hPa) fluorescence cell, where the OH radicals were electronically excited by tunable, pulsed UV laser radiation at a wavelength of 308 nm. The resulting OH resonance fluorescence was detected by time-delayed gated photon counting. The measurement system was calibrated using quantitative photolysis of water vapor in synthetic air at 185 nm as an OH source. For the PRD campaign, the limit of detection was  $(0.5\text{--}1) \times 10^6 \text{ cm}^{-3}$  at 5 min integration time and the accuracy was 20% ( $1\sigma$ ).

NO<sub>x</sub> and O<sub>3</sub> were measured by commercial instruments (Takegawa et al., 2006). NO was detected by NO-O<sub>3</sub> chemiluminescence (Thermo Electron, Model 42CTL), while NO<sub>2</sub> was first converted to NO in a photolytical reactor (Droplet Measurement Technologies, Model BLC). The instruments were calibrated using NO standard gas mixtures and gas phase titration for NO<sub>2</sub>. The 1-min detection limits for NO and NO<sub>2</sub> were 50 pptv and 170 pptv, respectively, and the corresponding accuracies were 7% and 13%. Ozone was measured using an ultraviolet (UV) absorption instrument (Thermo Electron, Model 49C) with a  $1\sigma$  precision of 0.3 ppb and an accuracy of 5%.

Title Page

Abstract

Introduction

Conclusions

References

Tables

Figures

◀

▶

◀

▶

Back

Close

Full Screen / Esc

Printer-friendly Version

Interactive Discussion



CO measurements were obtained by a NDIR gas analyzer (Thermo Electron, Model 48C) with an integration time of 1 min. Air samples were dried before measurement in order to avoid the interference from water vapour. The overall precision and accuracy were estimated to be 4 ppb and 20 ppb, respectively, at a CO mixing ratio of 400 ppb.

HONO was measured by a commercial instrument (QUMA, Wuppertal) using the LOPAP technique developed by Kleffmann et al. (2006). The instrument had a detection limit of 7 pptv at a time resolution of 5 min and the accuracy of calibration was estimated to be 10% ( $1\sigma$ ) (Li et al., 2009).

Measurements of alkanes, alkenes and aromatic compounds were performed using an automated gas chromatograph (Agilent, Model 6890 GC) equipped with dual columns and dual flame ionization detectors (Wang et al., 2008). Two sorbent traps were packed with different molecular sieves for a different range of VOCs. A porous-layer open tubular (PLOT)  $\text{Al}_2\text{O}_3/\text{KCl}$  column (Hewlett Packard) separated  $\text{C}_3\text{-C}_6$  and a DB-1 column (J&W)  $\text{C}_6\text{-C}_{12}$ . Calibration was performed by injecting various amounts of gas standard mixture containing the 51 target species with concentrations in the range between 3 ppb and 15 ppb (Spectra gas, Branchburg, NJ, USA). The accuracy for most of the measured VOCs estimated by comparing two traceable gas standards (68 C2-C11 NMHCs, Scott Marrin Inc.; 57 C2-C12 NMHCs, Spectra Gases Inc., USA) is within 10%. The time resolution was one hour, the precisions mostly 1–3% and detection limits 6–70 pptv.

Photolysis frequencies were calculated from solar actinic-flux spectra measured with a spectroradiometer (Meteorologie Consult) (Bohn et al., 2008). The radiometer was calibrated with a PTB-traceable irradiance standard before and after the campaign. The accuracy of derived photolysis frequencies is estimated to be about 10% at solar zenith angles smaller than  $80^\circ$ .

**OH reactivity  
measurement**

S. Lou et al.

Title Page

Abstract

Introduction

Conclusions

References

Tables

Figures

I◀

▶I

◀

▶

Back

Close

Full Screen / Esc

Printer-friendly Version

Interactive Discussion



## 4 Model calculations

A zero-dimensional chemical model was used to calculate concentrations of radicals and photochemical products of nitrogen and carbon compounds. The model (Rohrer and Berresheim, 2006; Hofzumahaus et al., 2009) was based on the Regional Atmospheric Chemical Mechanism (RACM) (Stockwell et al., 1997) upgraded with an improved isoprene chemistry (Karl et al., 2006). The calculations were constrained to measurements of O<sub>3</sub>, HONO, NO, NO<sub>2</sub>, CO, C<sub>3</sub>-C<sub>12</sub> VOCs, photolysis frequencies, water vapor, ambient temperature and pressure (Table 2). Concentrations of ethane and ethene were set to fixed values of 1.5 ppb and 3 ppb, respectively, estimated from a few canister samples. CH<sub>4</sub> and H<sub>2</sub> mixing ratios were assumed to be 1900 ppb and 550 ppb, respectively. The model was operated in a time-dependent mode with 5 min time resolution and 2 days spin-up time. Additional loss by deposition with a corresponding lifetime of 24 h for calculated species was assumed to avoid build-up of unrealistic amounts of secondary products. Some additional model runs were performed as sensitivity studies. First, OH was used as an additional constraint. Second, the assumed value of the deposition lifetime for calculated species was varied. Details and results of the sensitivity runs are given below.

## 5 Results

### 5.1 Measurements

$k_{\text{OH}}$  measurements are presented in Fig. 2 together with the measured concentrations of four selected trace gases (CO, NO<sub>2</sub>, propene, isoprene) that react with OH. The time series of  $k_{\text{OH}}$  has two major breaks which were caused by rainy weather conditions during typhoon Bilis on 15–18 July and an electrical power blackout at Backgarden on 22 July. The OH reactivity data exhibit diurnal patterns which are most clearly pronounced during the sunny period from 19 to 25 July, with daily  $k_{\text{OH}}$  minima between 10 s<sup>-1</sup> and

Title Page

Abstract

Introduction

Conclusions

References

Tables

Figures

◀

▶

◀

▶

Back

Close

Full Screen / Esc

Printer-friendly Version

Interactive Discussion



**OH reactivity  
measurement**

S. Lou et al.

Title Page

Abstract

Introduction

Conclusions

References

Tables

Figures

◀

▶

◀

▶

Back

Close

Full Screen / Esc

Printer-friendly Version

Interactive Discussion



30 s<sup>-1</sup> at noontime and peak values up to 120 s<sup>-1</sup> at night. The temporal pattern is highly correlated with variations of anthropogenically emitted pollutants like CO, NO<sub>2</sub> and propene (Fig. 2, lower panels). The pollutants accumulated in the shallow nocturnal boundary layer and were reduced by photochemical degradation and vertical mixing within the rising boundary layer during daytime. Isoprene, which is emitted mostly by plants, behaved differently and reached maximum values in the late afternoon as it is expected from its temperature dependent emission rate. The observed isoprene (up to 5 ppb, equivalent to an OH reactivity of up to 12 s<sup>-1</sup>) made a significant contribution to  $k_{\text{OH}}$ , but the variations of isoprene are not clearly discernible in  $k_{\text{OH}}$  which was dominated by the diurnal cycle of anthropogenic pollutants.

On two days (24–25 July) the  $k_{\text{OH}}$  data appear to be more scattered than on other days. The rather large short-term variability cannot be explained by instrumental noise, but was likely caused by local emissions in the surrounding neighborhood. Smoke plumes from small fires were observed on these days on agricultural fields nearby, where harvest residues were burnt during daytime. During the nights of 23/24 and 24/25 July, smell was noticeable that came presumably from waste combustion. Finally, before midnight from 25 to 26 July,  $k_{\text{OH}}$  dropped sharply by a factor of 3 coinciding with starting rain. The rain fall in the wake of typhoon Kaemi continued on the next day and kept the reactivity on a level of 20 s<sup>-1</sup>.

In order to test how well the measured  $k_{\text{OH}}$  can be explained by the measured set of trace gases, OH reactivities were calculated according to Eq. (2) using the compounds listed in Table 2. The corresponding rate coefficients were taken from the RACM model and were applied for the instrumental conditions of the  $k_{\text{OH}}$  measurements (1 atm, 313 K). The resulting  $k_{\text{OH}}^{\text{calc}}$  data correlate well with the measurements, but are lower on average by a factor of 2 (Fig. 3). The discrepancy is even larger on 25 and 26 July and reaches a factor of 3–4 before sunrise, when combustion smell was noticeable. In general, the differences between measured and calculated reactivities are significantly larger than the experimental error of  $k_{\text{OH}}$  (10%) and the estimated total uncertainty of  $k_{\text{OH}}^{\text{calc}}$  (20%), pointing to missing reactivity in the set of trace gas measurements.

**OH reactivity  
measurement**

S. Lou et al.

Title Page

Abstract

Introduction

Conclusions

References

Tables

Figures

◀

▶

◀

▶

Back

Close

Full Screen / Esc

Printer-friendly Version

Interactive Discussion



The measured  $k_{\text{OH}}$  data and their mean diurnal variation are displayed in Fig. 4 (upper panel) showing a minimum mean value of  $20 \text{ s}^{-1}$  at local noon and a maximum mean value of  $50 \text{ s}^{-1}$  at daybreak. The relative contributions of measured  $\text{CO}$ ,  $\text{NO}_x$  and hydrocarbons are shown in the lower panel of Fig. 4. Interestingly, their cumulated contribution (black squared symbols) is nearly independent of time and explains half of the measured OH reactivity. The largest fraction of the explained reactivity comes from the group of measured VOCs which are further analyzed in Fig. 5. Here, the dominating speciated VOC reactivities are displayed versus time, normalized to the total reactivity of all measured hydrocarbons. Apparently, isoprene was the most important measured OH reactant during daytime, with a contribution up to 70% of the total hydrocarbon reactivity, whereas simple alkenes (propene, butenes, pentenes) and aromatic compounds (styrene, toluene, xylenes and trimethylbenzenes) were dominating at night.

The question arises, which atmospheric components were responsible for the missing 50% of OH reactivity that is not explained by measured  $\text{CO}$ ,  $\text{NO}_x$  and hydrocarbons. Other compounds that were measured ( $\text{O}_3$ , HONO,  $\text{SO}_2$ ,  $\text{H}_2\text{O}_2$  and  $\text{CH}_3\text{OOH}$ ), but not included in  $k_{\text{OH}}^{\text{calc}}$ , cannot explain the discrepancy, as their cumulated contribution is on average less than  $1 \text{ s}^{-1}$  and therefore negligible. The missing reactivity must be due to unmeasured primary reactants which were emitted by anthropogenic or biogenic sources, or to unmeasured chemical species that have been formed photochemically in the atmosphere. These possibilities are discussed below.

## 5.2 Model results

In order to estimate the possible contribution of unmeasured, secondary pollutants to the missing OH reactivity, a photochemical box model (RACM) was applied (Sect. 4). Total OH reactivities ( $k_{\text{OH}}^{\text{model}}$ ) were calculated from measured trace gases and all model-generated products, assuming instrumental conditions (1 atm, 313 K) for the OH rate coefficients. The resulting model-derived reactivities are higher than  $k_{\text{OH}}^{\text{calc}}$  by a fac-

tor of 1.4–2.6. They exhibit a similar good correlation to measured  $k_{\text{OH}}$  as  $k_{\text{OH}}^{\text{calc}}$ , but are in much better absolute agreement with the observations (Fig. 3). The model results agree well with the observed reactivities during daytime (except on 24 July, noon), but still underestimate the observations at night. The general trend can be seen more clearly in Fig. 6 (lower panel), where the mean diurnal profile of the modelled-to-measured  $k_{\text{OH}}$  ratio is displayed. From 08:00 to 17:00 CNST the model and measurement results agree within  $\pm 10\%$ . At night, however, the model underpredicts the measured reactivity systematically, with the largest discrepancy of 30% at sunrise.

## 6 Discussion

### 6.1 $k_{\text{OH}}$ measurements

The OH reactivities observed at Backgarden ( $10\text{--}120\text{ s}^{-1}$ ) are among the highest ever measured in field campaigns (Table 1). While clean air can have a reactivity as low as  $\sim 1\text{ s}^{-1}$  in the remote marine boundary layer (Brauers et al., 2001), highest  $k_{\text{OH}}$  values have been measured in polluted megacities with reported values of  $10\text{--}200\text{ s}^{-1}$  in Mexico City (Shirley et al., 2006) and  $10\text{--}100\text{ s}^{-1}$  in Tokyo (Sadanaga et al., 2005; Yoshino et al., 2006) and New York City (Ren et al., 2003a, 2006a). Maximum values in Mexico City and New York City were observed during the morning and evening rush-hours, while minimum reactivities with mean values of  $20\text{--}25\text{ s}^{-1}$  were measured in the afternoon at pollution levels of typ.  $20\text{ ppb NO}_x$ . High reactivities reaching about  $60\text{ s}^{-1}$  were also observed in the tropical rainforest of Suriname (Sinha et al., 2008) and Borneo (Ingham et al., 2009), where natural emissions of isoprene and possible other biogenic VOCs dominated the OH reactivity.

The situation at the rural site in PRD is rather complex as it was strongly influenced by both anthropogenic and biogenic emissions. At night, the mean OH reactivity had values between  $35\text{ s}^{-1}$  and  $50\text{ s}^{-1}$  which were dominated by anthropogenic pollutants (Figs. 4 and 5). In the afternoon, the mean reactivity was about  $20\text{ s}^{-1}$ , which is similar

Title Page

Abstract

Introduction

Conclusions

References

Tables

Figures

◀

▶

◀

▶

Back

Close

Full Screen / Esc

Printer-friendly Version

Interactive Discussion



to the observed values in New York and Mexico City. However, unlike in these cities, the afternoon values at PRD were biogenically influenced by several ppb of isoprene at relatively low  $\text{NO}_x$  (1–2 ppb). As mentioned above, about half of the observed reactivity at PRD can be explained by measured CO,  $\text{NO}_x$  and hydrocarbons, of which isoprene, light alkenes and aromatics make the largest contributions to the explained reactivity.

The high CO and  $\text{NO}_x$  concentrations at night were probably caused by local combustion of coal for cooking and heating purposes, and presumably burning of waste and biomass. Furthermore, advected traffic emissions were strongly enhanced at night (Garland et al., 2008), as a result of local traffic regulations banning heavy Diesel trucks during daytime from 07:00 to 21:00 CNST (Bradsher, 2007).

VOCs can have many sources in PRD (Liu et al., 2008b). The possible origin of light monoalkenes is from car traffic and biomass burning, and aromatic compounds may come from traffic exhaust, painting and industrial use of solvents. Isoprene is predominantly a biogenic tracer, but can also be a product of biomass burning and car exhausts (Liu et al., 2008b).

## 6.2 Missing reactivity

The missing reactivity identified in Figs. 3 and 4 may come from unmeasured primary reactants emitted by anthropogenic or biogenic sources, or from unmeasured chemical species that were photochemically produced in the atmosphere. The good agreement between the modelled (base case) and measured reactivities during the time from 08:00 to 17:00 CNST (Figs. 3 and 6, lower panel) suggests that photochemically formed products can explain the missing OH reactivity at daytime. The chemical partitioning of the modelled reactivity indicates that formaldehyde, higher aldehydes (ALD) and oxygenated isoprene products (OISO) are probably the most important OH reactants among the unmeasured, photochemical products (Fig. 6, upper panel). These oxidation products contribute 30–40% and other organic compounds (ketones, dicarbonyl compounds, alcohols, hydroperoxides, nitrates etc.) 10–20% of the total OH reactivity. Overall, organic species dominated  $k_{\text{OH}}$  and explain up to 85% (15:00 CNST)

Title Page

Abstract

Introduction

Conclusions

References

Tables

Figures

◀

▶

◀

▶

Back

Close

Full Screen / Esc

Printer-friendly Version

Interactive Discussion



of the measured OH reactivity at daytime. It is noteworthy that isoprene (17%) and its oxidation products OISO (24%) played a prominent role in the afternoon, accounting for about 40% of the total reactivity.

A large contribution of aldehydes and oxygenated VOCs (OVOCs) to atmospheric reactivity was also reported in other studies, including various environments (Shao et al., 2009; Steiner et al., 2008; Emmerson et al., 2007; Yoshino et al., 2006; Lewis et al., 2005). In Central California, US, Steiner et al. (2008) compared VOC reactivities from the regional Community Multiscale Air Quality model (CMAQ) with calculated reactivities for urban and agricultural measurement stations. In general, aldehydes and other OVOCs were found to contribute 30–50 % of the modelled urban VOC reactivity (up to  $30 \text{ s}^{-1}$ ), while OVOCs did account for up to 90% of the modelled reactivity in agricultural regions. In an urban study, Yoshino et al. (2006) analyzed OH reactivities measured in Tokyo at different seasons. In summer, measured hydrocarbons and OVOCs could explain 26% and 14% of the total reactivity, respectively. A missing reactivity of 25% was ascribed to unmeasured OVOCs summing up to an estimated total OVOC fraction of 39%. At wintertime, hydrocarbons did account for 25%, OVOCs for 3–4%, and unmeasured compounds for 5% of the total reactivity. These numbers indicate much smaller photochemical activity and less production of oxygenated VOCs in winter (Yoshino et al., 2006). Detailed speciated measurements of VOCs and OVOCs were obtained at summertime in Beijing by Shao et al. (2009), analyzing the partitioning of the organic reactivity and its impact on photochemical ozone formation. The most abundant OVOCs were formaldehyde, acetaldehyde, acetone, methanol and ethanol, contributing in total about 40% of the calculated organic reactivity. The measured diurnal pattern of acetaldehyde revealed that aldehydes were mostly photochemically formed (Shao et al., 2009). An essential role of OVOCs was also demonstrated in the TORCH campaign in south-east England in summer 2003, where aldehydes were not only an important sink of OH, but also a significant photolytical source of  $\text{HO}_x$  (Emmerson et al., 2007). Even in relatively clean environments, OVOCs were found to play a significant role. Lewis et al. (2005) report observations of organic species at a re-

**OH reactivity  
measurement**

S. Lou et al.

Title Page

Abstract

Introduction

Conclusions

References

Tables

Figures

◀

▶

◀

▶

Back

Close

Full Screen / Esc

Printer-friendly Version

Interactive Discussion



**OH reactivity  
measurement**

S. Lou et al.

Title Page

Abstract

Introduction

Conclusions

References

Tables

Figures

I◀

▶I

◀

▶

Back

Close

Full Screen / Esc

Printer-friendly Version

Interactive Discussion



mote observatory (Mace-Head) at the North-Atlantic coast of Ireland, where acetone, methanol and acetaldehyde contributed up to 80% of the calculated organic reactivity. Their data analysis demonstrates that a large fraction of OVOCs was formed by secondary chemistry in the background atmosphere. Airborne measurements of atmospheric reactants over the relatively clean Pacific Ocean have shown a contribution of about 20% of OVOCs to the loss rate of OH (Mao et al., 2009). Direct  $k_{\text{OH}}$  measurements in the lower 2 km, however, indicate a missing reactivity of more than a factor of 2, suggesting that some highly reactive VOCs had not been measured (Mao et al., 2009).

In the present study, the box model underestimates systematically the measured OH reactivity at night and in the early morning by as much as 30% on average (Figs. 3 and 4). The discrepancies may be caused by systematic model errors (see below) or indicate unmeasured reactive emissions that are not captured by the model. Unknown emissions are the most likely cause of the large differences that occur during the nights of 24 and 25 July, when combustion smell was clearly noticeable at the measurement site. As the burning material and the combustion conditions are not known, it is difficult to specify the emitted pollutants. A multitude of reactants can be emitted by combustion of organic materials, including various OVOCs, semivolatile organic compounds (SVOC), polyaromatic hydrocarbons (PAHs), halogen and nitrogen containing organic species (Andreae and Merlet, 2001; Lemieux et al., 2004), all of which were not measured in this field study.

### 6.3 Model uncertainty

Given a missing reactivity of a factor 2, it is surprising how well the RACM model reproduces the observed OH reactivity at daytime (Fig. 6, lower panel). Apparently, the model produces the right amount of OVOCs and other oxidation products to fill the gap between the calculated and measured reactivity. It is an interesting question, whether the good agreement at daytime is just fortuitous and whether the systematic underestimation of  $k_{\text{OH}}$  by the model at night is significant.

**OH reactivity  
measurement**

S. Lou et al.

The error of the model is at least as large as that of  $k_{\text{OH}}^{\text{calc}}$  ( $\pm 20\%$ ), which is determined by the measured air components and the corresponding rate constants. Additional uncertainty is caused by the reactivity of the modelled oxidation products. There are two main shortcomings of the model that increase the uncertainty. One is the simplified treatment of product loss by transport, assuming a fixed lifetime of 24 h for deposition of all calculated species in the model. This lifetime is equivalent to an assumed deposition velocity of 1.2 cm/s and a boundary layer height of 1000 m. The simplified treatment ignores the variability of the atmospheric boundary layer, wet deposition by rain events, and differences in the deposition velocities of different species. The other shortcoming is the inability of the model to reproduce afternoon OH concentrations which were measured together with  $k_{\text{OH}}$  at Backgarden. Hofzumahaus et al. (2009) found that the same model is capable of describing measured OH at  $\text{NO} > 1$  ppb in the morning, but underestimates the observed OH,  $(1-2) \times 10^7$  radicals per  $\text{cm}^3$ , by a factor 3–5 at NO levels of 0.1–0.2 ppb in the afternoon. This shortcoming influences the predicted concentrations of secondary products which are produced by OH oxidation of VOCs.

Tests were performed to estimate the sensitivity of  $k_{\text{OH}}^{\text{model}}$  to the assumed deposition lifetime and OH concentration, varying the two parameters independently by a factor 2 as model input. In case of OH, twice and half of the modelled OH from the base run was prescribed as model input for the sensitivity runs. The resulting time series of  $k_{\text{OH}}^{\text{model}}$  look very similar to the base case upon variation of the OH concentration (Fig. 7, upper panel) and deposition lifetime (Fig. 7, lower panel). In both cases, the modified model yields oxidation product reactivities which are 10–30% different, causing only marginal differences (5–15%) in the total OH reactivity. As a further test, the model was constrained by the measured OH concentrations. On average the modelled reactivity increases by 30%, improving the agreement with the observed nighttime reactivities. Daytime values of  $k_{\text{OH}}^{\text{model}}$  show relatively small changes on particular days (e.g. on 20, 21, 23 and 26 July) and remain in good agreement with the measurements. However,  $k_{\text{OH}}$  is considerably overpredicted by the model on three days at noon, by a factor 1.5 on 13 and 25 July, and a factor 2 on 24 July. The episodic overprediction shows that

[Title Page](#)[Abstract](#)[Introduction](#)[Conclusions](#)[References](#)[Tables](#)[Figures](#)[◀](#)[▶](#)[◀](#)[▶](#)[Back](#)[Close](#)[Full Screen / Esc](#)[Printer-friendly Version](#)[Interactive Discussion](#)

the prediction of secondary product reactivities by the simple box model can have a rather large error. This may be due to an overprediction of the production of oxidized species by the RACM mechanism for the atmospheric composition at PRD, or by a deposition rate which is larger for polar, oxygenated species than assumed in this study.

5 In conclusion, most differences between modelled and measured OH reactivities are not likely significant with respect to the model uncertainty, except for the very high reactivities observed at midnight.

## 7 Conclusions

10 Total atmospheric OH reactivities have been measured by a newly developed instrument at a rural site in the densely populated Pearl River Delta in Southern China in summer 2006. The deployed instrument uses laser flash photolysis of ozone to produce pulses of OH in samples of ambient air and applies laser-induced fluorescence to monitor the time-dependent decay of laser-generated OH. The experimental reactivities were derived as inverse chemical OH lifetimes with a total accuracy of about 10%  
15 at a time resolution of 1–3 min. In addition, a comprehensive set of atmospheric trace gases and meteorological parameters was measured.

The observed OH reactivities are among the highest ever reported by direct methods (Table 1), spanning a range from  $10\text{ s}^{-1}$  to  $120\text{ s}^{-1}$ . On average, the reactivities exhibited a clear diurnal profile with a mean maximum value of  $50\text{ s}^{-1}$  at daybreak and a mean minimum value of  $20\text{ s}^{-1}$  at noon. The magnitude of these values and their diurnal variation is similar to what has been observed by other research groups in New York, Tokyo, or Mexico City, which are highly polluted, anthropogenically influenced places. The measurement site in this study, however, was a green, rural site in the densely populated PRD. The OH reactivity was characterized by a background of  
20 anthropogenic pollutants at night and was dominated by local, biogenic emissions of isoprene during the day.  
25

Title Page

Abstract

Introduction

Conclusions

References

Tables

Figures

◀

▶

◀

▶

Back

Close

Full Screen / Esc

Printer-friendly Version

Interactive Discussion



**OH reactivity  
measurement**

S. Lou et al.

[Title Page](#)[Abstract](#)[Introduction](#)[Conclusions](#)[References](#)[Tables](#)[Figures](#)[I◀](#)[▶I](#)[◀](#)[▶](#)[Back](#)[Close](#)[Full Screen / Esc](#)[Printer-friendly Version](#)[Interactive Discussion](#)

The comparison of reactivities calculated from measured CO, NO<sub>x</sub> and hydrocarbons with measured  $k_{\text{OH}}$  has revealed a missing reactivity of unmeasured species of about a factor of 2 at day and night. Box model calculations suggest that the missing reactivity is mainly contributed by OVOCs that were photochemically formed by oxidation of hydrocarbons. Despite the simplicity of the model, the agreement between measured and modelled  $k_{\text{OH}}$  is surprisingly good and robust in view of the model assumptions. The model reproduces the observed, time-dependent variability of  $k_{\text{OH}}$  and agrees within 10% at daytime, but underpredicts the measured nighttime values by 30%. If the model is additionally constrained by the measured concentrations of OH, agreement at night is improved, but daytime values become episodically overpredicted. Thus, the general differences between modelled and measured  $k_{\text{OH}}$  cannot be considered as significant with respect to the model uncertainty.

Based on the measured trace gases and model calculated secondary products,  $k_{\text{OH}}$  was found to be dominated by VOCs and OVOCs, with a maximum total organic contribution of 85% in the afternoon. The major VOCs were light alkenes and aromatics at night and isoprene during day. According to the model, aldehydes and oxidized isoprene products were the dominating OVOC species, having a larger share of reactivity than the hydrocarbons at daytime. The important role of OVOCs was also recognized in other studies, analyzing atmospheric OH reactivities in marine, rural and urban air (see discussion in Sect. 6.2 above). In these environments, the OVOC reactivity was often of similar magnitude as that of hydrocarbons, if conditions were favoring photochemical oxidation of VOCs. This common result emphasizes the need for widespread OVOC measurements of high data quality, but, at present, such measurements are not generally available on a routine basis (Apel et al., 2008). Improved measurement techniques for organic species and further measurements of atmospheric OH reactivities will be needed to make further progress in understanding tropospheric chemistry and its role in photochemical formation of ozone and aerosols.

*Acknowledgements.* We thank the PRiDe PRD2006 campaign team (2002CB410801), especially M. Hu, N. Takegawa, and A. Oebel for help and support at the field site. C. C. thanks Academic Sinica, Taiwan, for financial support of this work.

## References

- 5 Andreae, M. O. and Merlet, P.: Emission of trace gases and aerosols from biomass burning, *Global Biogeochem. Cy.*, 15, 955–966, 2001. 17052
- Apel, E. C., Brauers, T., Koppmann, R., Bandowe, B., Boßmeyer, J., Holzke, C., Tillmann, R., Wahner, A., Wegener, R., Brunner, A., Jocher, M., Ruuskanen, T., Spirig, C., Steigner, D., Steinbrecher, R., Alvarez, E. G., Müller, K., Burrows, J. P., Schade, G., Solomon, S. J.,  
10 Ladstätter-Weißemayer, A., Simmonds, P., Young, D., Hopkins, J. R., Lewis, A. C., Legreid, G., Reimann, S., Hansel, A., Wisthaler, A., Blake, R. S., Ellis, A. M., Monks, P. S., and Wyche, K. P.: Intercomparison of oxygenated volatile organic compound measurements at the SAPHIR atmosphere simulation chamber, *J. Geophys. Res.*, 113, D20307, doi:10.1029/2008JD009865, 2008. 17055
- 15 Bohn, B., Corlett, G. K., Gillmann, M., Sanghavi, S., Stange, G., Tensing, E., Vrekoussis, M., Bloss, W. J., Clapp, L. J., Kortner, M., Dorn, H.-P., Monks, P. S., Platt, U., Plass-Dülmer, C., Mihalopoulos, N., Heard, D. E., Clemmshaw, K. C., Meixner, F. X., Prevot, A. S. H., and Schmitt, R.: Photolysis frequency measurement techniques: results of a comparison within the ACCENT project, *Atmos. Chem. Phys.*, 8, 5373–5391, 2008,  
20 <http://www.atmos-chem-phys.net/8/5373/2008/>. 17045
- Bradsher, K.: Trucks Power China's Economy, at a Suffocating Cost, *The New York Times* – Online Edition, N.Y., 8 December 2007. 17050
- Brasseur, G. P., Prinn, R. G., and Pszenny, A. P. (Eds.): *Atmospheric Chemistry in a Changing World*, The IGBP Series, Springer, Berlin, 2003. 17037
- 25 Brauers, T., Hausmann, M., Bister, A., Kraus, A., and Dorn, H.-P.: OH radicals in the boundary layer of the Atlantic Ocean 1. Measurements by long-path absorption spectroscopy, *J. Geophys. Res.*, 106, 7399–7414, 2001. 17049
- Calpini, B., Jeanneret, F., Bourqui, M., Clappier, A., Vajtai, R., and van den Bergh, H.: Direct measurement of the total reaction rate of OH in the atmosphere, *Analisis*, 27, 328–336,  
30 1999. 17039, 17041

## OH reactivity measurement

S. Lou et al.

Title Page

Abstract

Introduction

Conclusions

References

Tables

Figures

◀

▶

◀

▶

Back

Close

Full Screen / Esc

Printer-friendly Version

Interactive Discussion



- Chan, C. K. and Yao, X.: Air pollution in mega cities in China, *Atmos. Environ.*, 42, 1–42, 2008. 17040, 17041
- Di Carlo, P., Brune, W. H., Martinez, M., Harder, H., Leshner, R., Ren, X., Thornberry, T., Carroll, M. A., Young, V., Shepson, P. B., Riemer, D., Apel, E., and Campbell, C.: Missing OH Reactivity in a Forest: Evidence for Unknown Reactive Biogenic VOCs, *Science*, 304, 722–724, 2004. 17038, 17064
- Ehhalt, D. H.: Photooxidation of trace gases in the troposphere, *Phys. Chem. Chem. Phys.*, 1, 5401–5408, 1999. 17036
- Emmerson, K. M., Carslaw, N., Carslaw, D. C., Lee, J. D., McFiggans, G., Bloss, W. J., Gravesstock, T., Heard, D. E., Hopkins, J., Ingham, T., Pilling, M. J., Smith, S. C., Jacob, M., and Monks, P. S.: Free radical modelling studies during the UK TORCH Campaign in Summer 2003, *Atmos. Chem. Phys.*, 7, 167–181, 2007, <http://www.atmos-chem-phys.net/7/167/2007/>. 17051
- Garland, R. M., Yang, H., Schmid, O., Rose, D., Nowak, A., Achtert, P., Wiedensohler, A., Takegawa, N., Kita, K., Miyazaki, Y., Kondo, Y., Hu, M., Shao, M., Zeng, L. M., Zhang, Y. H., Andreae, M. O., and Pöschl, U.: Aerosol optical properties in a rural environment near the mega-city Guangzhou, China: implications for regional air pollution, radiative forcing and remote sensing, *Atmos. Chem. Phys.*, 8, 5161–5186, 2008, <http://www.atmos-chem-phys.net/8/5161/2008/>. 17041, 17050
- Goldstein, A. H. and Galbally, I. E.: Known and Unexplored Organic Constituents in the Earth's Atmosphere, *Environ. Sci. Technol.*, 41, 1514–1521, 2007. 17038
- Heald, C. L., Goldstein, A. H., Allan, J. D., Aiken, A. C., Apel, E., Atlas, E. L., Baker, A. K., Bates, T. S., Beyersdorf, A. J., Blake, D. R., Campos, T., Coe, H., Crouse, J. D., DeCarlo, P. F., de Gouw, J. A., Dunlea, E. J., Flocke, F. M., Fried, A., Goldan, P., Griffin, R. J., Herndon, S. C., Holloway, J. S., Holzinger, R., Jimenez, J. L., Junkermann, W., Kuster, W. C., Lewis, A. C., Meinardi, S., Millet, D. B., Onasch, T., Polidori, A., Quinn, P. K., Riemer, D. D., Roberts, J. M., Salcedo, D., Sive, B., Swanson, A. L., Talbot, R., Warneke, C., Weber, R. J., Weibring, P., Wennberg, P. O., Worsnop, D. R., Wittig, A. E., Zhang, R., Zheng, J., and Zheng, W.: Total observed organic carbon (TOOC) in the atmosphere: a synthesis of North American observations, *Atmos. Chem. Phys.*, 8, 2007–2025, 2008, <http://www.atmos-chem-phys.net/8/2007/2008/>. 17038
- Hofzumahaus, A., Rohrer, F., Lu, K., Bohn, B., Brauers, T., Chang, C. C., Fuchs, H., Holland, F., Kita, K., Kondo, Y., Li, X., Lou, S., Shao, M., Zeng, L., Wahner, A., and Zhang, Y.: Amplified

**OH reactivity  
measurement**

S. Lou et al.

Title Page

Abstract

Introduction

Conclusions

References

Tables

Figures

◀

▶

◀

▶

Back

Close

Full Screen / Esc

Printer-friendly Version

Interactive Discussion



- Trace Gas Removal in the Troposphere, *Science*, 324, 1702–1704, 2009. 17039, 17040, 17041, 17043, 17044, 17046, 17053, 17065
- Holland, F., Hofzumahaus, A., Schäfer, J., Kraus, A., and Pätz, H.-W.: Measurements of OH and HO<sub>2</sub> radical concentrations and photolysis frequencies during BERLIOZ, *J. Geophys. Res.*, 108, 8246, doi:10.1029/2001, 2003. 17042, 17044
- 5 Holzinger, R., Lee, A., Paw, K. T., and Goldstein, U. A. H.: Observations of oxidation products above a forest imply biogenic emissions of very reactive compounds, *Atmos. Chem. Phys.*, 5, 67–75, 2005, <http://www.atmos-chem-phys.net/5/67/2005/>. 17038
- 10 Hua, W., Chen, Z. M., Jie, C. Y., Kondo, Y., Hofzumahaus, A., Takegawa, N., Chang, C. C., Lu, K. D., Miyazaki, Y., Kita, K., Wang, H. L., Zhang, Y. H., and Hu, M.: Atmospheric hydrogen peroxide and organic hydroperoxides during PRIDE-PRD'06, China: their concentration, formation mechanism and contribution to secondary aerosols, *Atmos. Chem. Phys.*, 8, 6755–6773, 2008, <http://www.atmos-chem-phys.net/8/6755/2008/>. 17041, 17065
- 15 Ingham, T., Goddard, A., Whalley, L. K., Furneaux, K. L., Edwards, P. M., Seal, C. P., Self, D. E., Johnson, G. P., Read, K. A., Lee, J. D., and Heard, D. E.: A flow-tube based laser-induced fluorescence instrument to measure OH reactivity in the troposphere, *Atmos. Meas. Tech. Discuss.*, 2, 621–657, 2009, <http://www.atmos-meas-tech-discuss.net/2/621/2009/>. 17039, 17044, 17049, 17064
- 20 Karl, M., Dorn, H.-P., Holland, F., Koppmann, R., Poppe, D., Rupp, L., Schaub, A., and Wahner, A.: Product study of the reaction of OH radicals with isoprene in the atmosphere simulation chamber SAPHIR, *J. Atmos. Chem.*, 55, 167–187, 2006. 17046
- Kleffmann, J., Lörzer, J., Wiesen, P., Kern, C., Trick, S., Volkamer, R., Rodenas, M., and Wirtz, K.: Intercomparison of the DOAS and LOPAP techniques for the detection of nitrous acid (HONO), *Atmos. Environ.*, 40, 3640–3652, 2006. 17045
- 25 Kovacs, T. A. and Brune, W. H.: Total OH Loss Rate Measurement, *J. Atmos. Chem.*, 39, 105–122, 2001. 17039
- Kovacs, T. A., Brune, W. H., Harder, H., Martinez, M., Simpas, J. B., Frost, G. J., Williams, E., Jobson, T., Stroud, C., Young, V., Fried, A., and Wert, B.: Direct measurement of urban OH reactivity during Nashville SOS in summer 1999, *J. Environ. Monitor.*, 5, 68–74, 2003. 17043, 17044, 17064
- 30

---

**OH reactivity  
measurement**S. Lou et al.

---

[Title Page](#)[Abstract](#)[Introduction](#)[Conclusions](#)[References](#)[Tables](#)[Figures](#)[◀](#)[▶](#)[◀](#)[▶](#)[Back](#)[Close](#)[Full Screen / Esc](#)[Printer-friendly Version](#)[Interactive Discussion](#)

**OH reactivity  
measurement**

S. Lou et al.

Title Page

Abstract

Introduction

Conclusions

References

Tables

Figures

◀

▶

◀

▶

Back

Close

Full Screen / Esc

Printer-friendly Version

Interactive Discussion



- Lemieux, P. M., Lutes, C. C., and Santoianni, D. A.: Emissions of organic air toxics from open burning: a comprehensive review, *Prog. Energ. Combust.*, 30, 1–32, 2004. 17052
- Lewis, A. C., Carslaw, N., Marriott, P. J., Klingshorn, R. M., Morrison, P., Lee, A. L., Bartle, K. D., and Pilling, M. J.: A larger pool of ozone-forming carbon compounds in urban atmospheres, *Nature*, 405, 778–781, 2000. 17038
- Lewis, A. C., Hopkins, J. R., Carpenter, L. J., Stanton, J., Read, K. A., and Pilling, M. J.: Sources and sinks of acetone, methanol, and acetaldehyde in North Atlantic marine air, *Atmos. Chem. Phys.*, 5, 1963–1974, 2005, <http://www.atmos-chem-phys.net/5/1963/2005/>. 17051
- Li, X., Brauers, T., Shao, M., Garland, R. M., Wagner, T., Deutschmann, T., and Wahner, A.: MAX-DOAS measurements in southern China: 1. automated aerosol profile retrieval using oxygen dimers absorptions, *Atmos. Chem. Phys. Discuss.*, 8, 17661–17690, 2008, <http://www.atmos-chem-phys-discuss.net/8/17661/2008/>. 17041
- Li, X., Brauers, T., Shao, M., et al.: Nitrous acid (HONO) in southern China: Observations and the daytime budget during PRIDE-PRD2006, *Atmos. Chem. Phys.*, in preparation, 2009. 17045
- Liu, X., Cheng, Y., Zhang, Y., Jung, J., Sugimoto, N., Chang, S. Y., Kim, Y. J., Fan, S., and Zeng, L.: Influences of relative humidity and particle chemical composition on aerosol scattering properties during the 2006 PRD campaign, *Atmos. Environ.*, 42, 1525–1536, 2008a. 17041
- Liu, Y., Shao, M., Fu, L., Lu, S., Zen, L., and Tang, D.: Source profiles of volatile organic compounds (VOCs) measured in China: Part I, *Atmos. Environ.*, 42, 6247–6260, 2008b. 17050
- Lou, S., Hofzumahaus, A., Holland, F., et al., et al.: Measurement of total OH reactivity in the atmosphere using a laser-photolysis laser-induced fluorescence technique, *Atmos. Meas. Tech.*, in preparation, 2009. 17042, 17043, 17044
- Mao, J., Ren, X., Brune, W. H., Olson, J. R., Crawford, J. H., Fried, A., Huey, L. G., Cohen, R. C., Heikes, B., Singh, H. B., Blake, D. R., Sachse, G. W., Diskin, G. S., Hall, S. R., and Shetter, R. E.: Airborne measurement of OH reactivity during INTEX-B, *Atmos. Chem. Phys.*, 9, 163–173, 2009, <http://www.atmos-chem-phys.net/9/163/2009/>. 17038, 17039, 17052, 17064
- Martinez, M., Harder, H., Kovacs, T. A., Simpas, J. B., Bassis, J., Leshner, R., Brune, W. H., Frost, G. J., Williams, E. J., Stroud, C. A., Jobson, B. T., Roberts, J. M., Hall, S. R., Shetter, R. E., Wert, B., Fried, A., Alicke, B., Stutz, J., Young, V. L., White, A. B., and Zamora,

**OH reactivity  
measurement**

S. Lou et al.

Title Page

Abstract

Introduction

Conclusions

References

Tables

Figures

◀

▶

◀

▶

Back

Close

Full Screen / Esc

Printer-friendly Version

Interactive Discussion



R. J.: OH and HO<sub>2</sub> concentrations, sources, and loss rates during the Southern Oxidants Study in Nashville, Tennessee, summer 1999, *J. Geophys. Res.*, 108, 4617, doi:10.1029/2003JD003551, 2003. 17039

Matsumi, Y., Comes, F. J., Hancock, G., Hofzumahaus, A., Hynes, A. J., Kawasaki, M., and Ravishankara, A. R.: Quantum yields for production of O(<sup>1</sup>D) in the ultraviolet photolysis of ozone: Recommendation based on evaluation of laboratory data, *J. Geophys. Res.*, 107(D3), 4024, doi:10.1029/2001JD000510, 2002. 17037

McKeen, S. A., Mount, G., Eisele, F., Williams, E., Harder, J., Goldan, P., Kuster, W., Liu, S. C., Baumann, K., Tanner, D., Fried, A., Sewell, S., Cantrell, C., and Shetter, R.: Photochemical modeling of hydroxyl and its relationship to other species and during the Tropospheric OH Photochemistry Experiment, *J. Geophys. Res.*, 102, 6467–6493, 1997. 17038

Poppe, D., Bauer, R., Brauers, T., Brüning, D., Callies, J., Dorn, H.-P., Hofzumahaus, A., Johnen, F. J., Khedim, A., Koppmann, R., London, H., Müller, K. P., Neuroth, R., Plass-Dülmer, C., Platt, U., Rohrer, F., Rudolph, J., Schmidt, U., Wallasch, M., and Ehhalt, D. H.: A comparison of measured OH concentrations with model calculations, *J. Geophys. Res.*, 99, 16633–16642, 1994. 17038

Ren, X., Harder, H., Martinez, M., Leshner, R. L., Oligier, A., Shirley, T., Adams, J., Simpas, J. B., and Brune, W. H.: HO<sub>x</sub> concentrations and OH reactivity observations in New York City during PMTACS-NY2001, *Atmos. Environ.*, 37, 3627–3637, 2003a. 17049, 17064

Ren, X., Harder, H., Martinez, M., Leshner, R. L., Oligier, A., Simpas, J. B., Brune, W. H., Schwab, J. J., Demerjian, K. L., He, Y., Zhou, X., and Gao, H.: OH and HO<sub>2</sub> Chemistry in the urban atmosphere of New York City, *Atmos. Environ.*, 37, 3639–3651, 2003b. 17039

Ren, X., Brune, W. H., Cantrell, C. A., Edwards, G. D., Shirley, T., Metcalf, A. R., and Leshner, R. L.: Hydroxyl and Peroxy Radical Chemistry in a Rural Area of Central Pennsylvania: Observations and Model Comparisons, *J. Atmos. Chem.*, 52, 231–257, 2005. 17039, 17064

Ren, X., Brune, W. H., Mao, J., Mitchell, M. J., Leshner, R. L., Simpas, J. B., Metcalf, A. R., Schwab, J. J., Cai, C., Li, Y., Demerjian, K. L., Felton, H. D., Boynton, G., Adams, A., Perry, J., He, Y., Zhou, X., and Hou, J.: Behavior of OH and HO<sub>2</sub> in the winter atmosphere in New York City, *Atmos. Environ.*, 40, S252–S263, 2006a. 17049, 17064

Ren, X., Brune, W. H., Oligier, A., Metcalf, A. R., Simpas, J. B., Shirley, T., Schwab, J. J., Bai, C., Roychowdhury, U., Li, Y., Cai, C., Demerjian, K. L., He, Y., Zhou, X., Gao, H., and Hou, J.: OH, HO<sub>2</sub>, and OH reactivity during the PMTACS-NY Whiteface Mountain 2002 campaign: Observations and model comparison, *J. Geophys. Res.*, 111, D10S03, doi:10.

**OH reactivity  
measurement**

S. Lou et al.

Title Page

Abstract

Introduction

Conclusions

References

Tables

Figures

◀

▶

◀

▶

Back

Close

Full Screen / Esc

Printer-friendly Version

Interactive Discussion



1029/2005JD006126, 2006b. 17039, 17064

Richter, A., Burrows, J. P., Nüß, H., Granier, C., and Niemeier, U.: Increase of tropospheric nitrogen dioxide over China observed from space, *Nature*, 437, 129–132, 2005. 17040

Rohrer, F. and Berresheim, H.: Strong correlation between levels of tropospheric hydroxyl radicals and solar ultraviolet radiation, *Nature*, 442, 184–187, 2006. 17046

Rose, D., Nowak, A., Achtert, P., Wiedensohler, A., Hu, M., Shao, M., Zhang, Y., Andreae, M. O., and Pöschl, U.: Cloud condensation nuclei in polluted air and biomass burning smoke near the mega-city Guangzhou, China - Part 1: Size-resolved measurements and implications for the modeling of aerosol particle hygroscopicity and CCN activity, *Atmos. Chem. Phys. Discuss.*, 8, 17343–17392, 2008, <http://www.atmos-chem-phys-discuss.net/8/17343/2008/>. 17041

Sadanaga, Y., Yoshino, A., Kato, S., Yoshioka, A., Watanabe, K., Miyakawa, Y., Hayashi, I., Matsumoto, J., Nishiyama, A., Akiyama, N., Kanaya, Y., and Kajii, Y.: The importance of NO<sub>2</sub> and volatile organic compounds in the urban air from the viewpoint of OH reactivity, *Geophys. Res. Lett.*, 31, L08102, doi:10.1029/2004GL019661, 2004a. 17064

Sadanaga, Y., Yoshino, A., Watanabe, K., Yoshioka, A., Wakazano, Y., Kanaya, Y., and Kajii, Y.: Development of a measurement system of OH reactivity in the atmosphere by using a laser-induced pump and probe technique, *Rev. Sci. Instrum.*, 75, 2648–2655, 2004b. 17039, 17041, 17044

Sadanaga, Y., Yoshino, A., Kato, S., and Kajii, Y.: Measurements of OH Reactivity and Photochemical Ozone Production in the Urban Atmosphere, *Environ. Sci. Technol.*, 39, 8847–8852, 2005. 17038, 17049

Shao, M., Tan, X., Zhang, Y., and Li, W.: City clusters in China: air and surface water pollution, *Front. Ecol. Environ.*, 4, 353–361, 2006. 17040

Shao, M., Lu, S., Liu, Y., Xie, X., Chang, C., Huang, S., and Chen, Z.: Volatile organic compounds measured in summer in Beijing and their role in ground-level ozone formation, *J. Geophys. Res.*, 114, D00G06, doi:10.1029/2008JD010863, 2009. 17051

Shirley, T. R., Brune, W. H., Ren, X., Mao, J., Leshner, R., Cardenas, B., Volkamer, R., Molina, L. T., Molina, M. J., Lamb, B., Velasco, E., Jobson, T., and Alexander, M.: Atmospheric oxidation in the Mexico City Metropolitan Area (MCMA) during April 2003, *Atmos. Chem. Phys.*, 6, 2753–2765, 2006, <http://www.atmos-chem-phys.net/6/2753/2006/>. 17039, 17043, 17049, 17064

**OH reactivity  
measurement**

S. Lou et al.

Title Page

Abstract

Introduction

Conclusions

References

Tables

Figures

◀

▶

◀

▶

Back

Close

Full Screen / Esc

Printer-friendly Version

Interactive Discussion



Sinha, V., Williams, J., Crowley, J. N., and Lelieveld, J.: The Comparative Reactivity Method - a new tool to measure total OH Reactivity in ambient air, *Atmos. Chem. Phys.*, 8, 2213–2227, 2008,

<http://www.atmos-chem-phys.net/8/2213/2008/>. 17039, 17043, 17049, 17064

5 Steiner, A. L., Cohen, R. C., Harley, R. A., Tonse, S., Millet, D. B., Schade, G. W., and Goldstein, A. H.: VOC reactivity in central California: comparing an air quality model to ground-based measurements, *Atmos. Chem. Phys.*, 8, 351–368, 2008,

<http://www.atmos-chem-phys.net/8/351/2008/>. 17051

10 Stockwell, W. R., Kirchner, F., Kuhn, M., and Seefeld, S.: A new mechanism for regional atmospheric chemistry modeling, *J. Geophys. Res.*, 102, 25847–25879, 1997. 17046

Takegawa, N., Miyakawa, T., Kondo, Y., Jimenez, J. L., Worsnop, D. R., and Fukuda, M.: Seasonal and diurnal variations of submicron organic aerosol in Tokyo observed using the Aerodyne Aerosol Mass Spectrometer, *J. Geophys. Res.*, 111, D11206, doi: 10.1029/2005JD006515, 2006. 17044

15 Tie, X., Brasseur, G. P., Zhao, C. S., Granier, C., Massie, S., Qin, Y., Wang, P. C., Wang, G., Yang, P. C., and Richter, A.: Chemical characterization of air pollution in Eastern China and the Eastern United States, *Atmos. Environ.*, 40, 2607–2625, 2006. 17040

Wang, J. L., Wang, C. H., Lai, C. H., Chang, C. C., Liu, Y., Zhang, Y., Liu, S., and Shao, M.: Characterization of ozone precursors in the Pearl River Delta by time series observation of non-methane hydrocarbons, *Atmos. Environ.*, 42(25), 6233–6246, 2008. 17045

20 Xiao, R., Takegawa, N., Kondo, Y., Miyazaki, Y., Miyakawa, T., Hu, M., Shao, M., Zeng, L. M., Hofzumahaus, A., Holland, F., Lu, K., Sugimoto, N., Zhao, Y., and Zhang, Y. H.: Formation of submicron sulfate and organic aerosols in the outflow from the urban region of the Pearl River Delta in China, *Atmos. Environ.*, 43, 3754–3763, 2009. 17041

25 Yoshino, A., Sadanaga, Y., Watanabe, K., Kato, S., Miyakawa, Y., Matsumoto, J., and Kajii, Y.: Measurement of total OH reactivity by laser-induced pump and probe technique – comprehensive observations in the urban atmosphere of Tokyo, *Atmos. Environ.*, 40, 7869–7881, 2006. 17049, 17051, 17064

30 Zhang, J., Wang, T., Chameides, W. L., Cardelino, C., Kwok, J., Blake, D. R., Ding, A., and So, K. L.: Ozone production and hydrocarbon reactivity in Hong Kong, Southern China, *Atmos. Chem. Phys.*, 7, 557–573, 2007,

<http://www.atmos-chem-phys.net/7/557/2007/>. 17040

Zhang, Y. H., Hu, M., Zhong, L. J., Cheng, Y. F., Zeng, L. M., Wang, X. S., Xiang, Y. R., Wang, J. L., Gao, D. F., Shao, M., Fan, S. J., and Liu, S. C.: Regional ozone pollution and observation-based approach for analyzing ozone-precursor relationship during the PRIDE-PRD2004 campaign, *Atmos. Environ.*, 42, 6203–6218, 2008a. 17040

5 Zhang, Y. H., Hu, M., Zhong, L. J., Wiedensohler, A., Liu, S. C., Andreae, M. O., Wang, W., and Fan, S. J.: Regional Integrated Experiments on Air Quality over Pearl River Delta 2004 (PRIDE-PRD2004): Overview, *Atmos. Environ.*, 42, 6157–6173, 2008b. 17040

10 Zhang, Y. H., Hu, M., Liu, S. C., et al.: Continuous efforts to investigate regional air pollution in the Pearl River Delta, China: PRiDe PRD2006 campaign, *Atmos. Chem. Phys.*, in preparation, 2009. 17040

**OH reactivity  
measurement**

S. Lou et al.

Title Page

Abstract

Introduction

Conclusions

References

Tables

Figures

◀

▶

◀

▶

Back

Close

Full Screen / Esc

Printer-friendly Version

Interactive Discussion



**Table 1.** OH reactivities measured in the atmospheric boundary layer.

Campaign	Site	Months, Year	Conditions	$k_{\text{OH}} (\text{s}^{-1})^{\text{a}}$	MR <sup>b</sup>	Reference
TORCH-2	Weybourne, Norfolk, UK	Apr–May 2004	Marine, Coast	2–10	$\lesssim 3$	Ingham et al. (2009)
INTEX-B	Pacific Ocean	Apr–May 2006	Marine, h=0–2 km <sup>d</sup>	4.0±1.0 <sup>c</sup>	2.5	Mao et al. (2009)
SOS	Nashville, US	Jun–Jul 1999	Urban	11.3±4.8 <sup>c</sup>	1.4	Kovacs et al. (2003)
PMTACS	New York, US	Jun–Aug 2001	Urban, Megacity	15–25	~1	Ren et al. (2003a)
–	Tokyo, Japan	Jul–Aug 2003	Urban, Megacity	25–85	$\leq 1.5$	Sadanaga et al. (2004a)
MILAGRO	Mexico City	Apr 2003	Urban, Megacity	10–200	–	Shirley et al. (2006)
TORCH-1	Essex, UK	Jul–Aug 2003	Urban	2–30	–	Ingham et al. (2009)
PMTACS	New York, US	Jan–Feb 2004	Urban, Megacity	10–100	$\leq 1.5$	Ren et al. (2006a)
–	Tokyo, Japan	Nov 2004	Urban, Megacity	10–100	~1	Yoshino et al. (2006)
–	Mainz, Germany	Aug 2005	Urban	6–18	–	Sinha et al. (2008)
PROPHET	Michigan, US	Jul–Aug 2000	Mixed Forest	1–12	~1.5	Di Carlo et al. (2004)
–	Pennsylvania, US	May–Jun 2002	Rural	2–10	–	Ren et al. (2005)
PMTACS	Whiteface-Mountain, US	Jul–Aug 2002	Rural, Forest	4–10	~1	Ren et al. (2006b)
–	Brownsberg, Suriname	Aug 2005	Tropics, Rainforest	53 <sup>e</sup>	~3	Sinha et al. (2008)
OP-3	Borneo, Malaysia	Apr–May 2008	Tropics, Rainforest	10–60	–	Ingham et al. (2009)
PRIDE-PRD2006	PRD, China	Jul 2006	Subtropics, Rural	10–120	~2	This Work

<sup>a</sup> Range of measured data. Measurements are ground-based unless otherwise noted.

<sup>b</sup> Missing reactivity (MR) expressed by the ratio  $k_{\text{OH}}/k_{\text{OH}}^{\text{calc}}$ .

<sup>c</sup> Median ± standard deviation.

<sup>d</sup> Measurements aboard an aircraft.

<sup>e</sup> Average value of two hours of measurements.

## OH reactivity measurement

S. Lou et al.

Title Page

Abstract

Introduction

Conclusions

References

Tables

Figures

◀

▶

◀

▶

Back

Close

Full Screen / Esc

Printer-friendly Version

Interactive Discussion



OH reactivity  
measurement

S. Lou et al.

Title Page

Abstract

Introduction

Conclusions

References

Tables

Figures

◀

▶

◀

▶

Back

Close

Full Screen / Esc

Printer-friendly Version

Interactive Discussion

**Table 2.** Atmospheric compounds used to calculate  $k_{\text{OH}}$  values.

Compound	Technique	Volume Mixing Ratio <sup>a</sup>	$k_{\text{OH}}^{\text{calc}b}$	$k_{\text{OH}}^{\text{model}c}$
OH	Laser induced fluorescence	$\leq 1$ ppt <sup>d</sup>	–	+ <sup>e</sup>
O <sub>3</sub>	UV photometry	<120 ppb (<0.2 s <sup>-1</sup> )	–	+
NO	Chemiluminescence	<30 ppb (<5.6 s <sup>-1</sup> )	+	+
NO <sub>2</sub>	Chemiluminescence	<40 ppb (<10 s <sup>-1</sup> )	+	+
HONO	LOPAP <sup>f</sup>	<5 ppb (<0.5 s <sup>-1</sup> )	–	+
CO	IR photometry	<4 ppm (<24 s <sup>-1</sup> )	+	+
H <sub>2</sub>	estimated	550 ppb (0.1 s <sup>-1</sup> ) <sup>g</sup>	+	+
CH <sub>4</sub>	estimated	1900 ppb (0.3 s <sup>-1</sup> ) <sup>g</sup>	+	+
C <sub>2</sub> H <sub>6</sub>	Canister sample – GC <sup>h</sup>	1.5 ppb (0.01 s <sup>-1</sup> ) <sup>g</sup>	+	+
C <sub>2</sub> H <sub>4</sub>	Canister sample – GC <sup>h</sup>	3 ppb (0.6 s <sup>-1</sup> ) <sup>g</sup>	+	+
C <sub>3</sub> –C <sub>12</sub> VOCs	Online – GC <sup>h</sup>	–	+	+
SO <sub>2</sub>	UV fluorescence	10 ppb (0.22 s <sup>-1</sup> ) <sup>i</sup>	–	–
H <sub>2</sub> O <sub>2</sub>	Derivatisation/HPLC <sup>k</sup>	0.75 ppb (0.03 s <sup>-1</sup> ) <sup>i</sup>	–	–
CH <sub>3</sub> OOH	Derivatisation/HPLC <sup>k</sup>	0.24 ppb (0.04 s <sup>-1</sup> ) <sup>i</sup>	–	–

<sup>a</sup> Numbers in paranthesis represent OH reactivities of the listed compounds at ambient conditions.

<sup>b</sup> Plus signs indicate the compounds included in  $k_{\text{OH}}^{\text{calc}}$ .

<sup>c</sup> Plus signs indicate the compounds used as model input for  $k_{\text{OH}}^{\text{model}}$ .

<sup>d</sup> Hofzumahaus et al. (2009).

<sup>e</sup> Used as model input in model sensitivity runs as explained in the text.

<sup>f</sup> Long-path absorption photometry.

<sup>g</sup> Fixed value (see text).

<sup>h</sup> Gas chromatography; see measured species in Table 3.

<sup>i</sup> Median value (Hua et al., 2008).

<sup>k</sup> High performance liquid chromatography.

OH reactivity  
measurement

S. Lou et al.

**Table 3.** Volatile organic compounds measured by online GC.

Class	Species
Alkanes	Propane, <i>n</i> -Butane, <i>i</i> -Butane, <i>n</i> -Pentane, <i>i</i> -Pentane, Cyclopentane, <i>n</i> -Hexane, 2-Methylpentane, 3-Methylpentane, 2,2-Dimethylbutane, 2,3-Dimethylbutane, Cyclohexane, Methylcyclopentane, <i>n</i> -Heptane, 2-Methylhexane, 3-Methylhexane, 2,3-Dimethylpentane, 2,4-Dimethylpentane, Methylcyclohexane, <i>n</i> -Octane, 2-Methylheptane, 3-Methylheptane, <i>n</i> -Nonane, <i>n</i> -Decane, <i>n</i> -Undecane, <i>n</i> -Dodecane
Alkenes	Propene, 1-Butene, <i>cis</i> -2-Butene, <i>trans</i> -2-Butene, 1-Pentene, <i>cis</i> -2-Pentene, <i>trans</i> -2-Pentene
Dienes	Isoprene
Aromatics	Benzene, Toluene, Ethylbenzene, <i>n</i> -Propylbenzene, <i>i</i> -Propylbenzene, <i>o</i> -Xylene, <i>m</i> -Xylene, <i>p</i> -Xylene, <i>o</i> -Ethyltoluene, <i>m</i> -Ethyltoluene, <i>p</i> -Ethyltoluene, Styrene, <i>m</i> -Diethylbenzene, <i>p</i> -Diethylbenzene, 1,2,3-Trimethylbenzene, 1,2,4-Trimethylbenzene, 1,3,5-Trimethylbenzene

Title Page

Abstract

Introduction

Conclusions

References

Tables

Figures

I◀

▶I

◀

▶

Back

Close

Full Screen / Esc

Printer-friendly Version

Interactive Discussion



OH reactivity  
measurement

S. Lou et al.

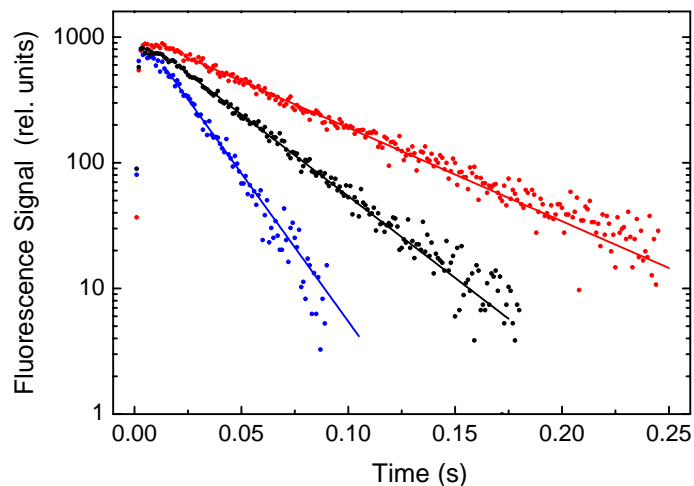


**Fig. 1.** OH decays measured in real-time by LIF in different samples of air at the Backgarden field site in PRD on 11 July 2006. Dots denote the measured time-dependent fluorescence signals recorded in time bins of 1 ms width, after an off-resonance background signal (ca. 1–2 rel. units) has been subtracted. The solid lines are exponential fits to the decay curves, yielding OH reactivities as reciprocal  $1/e$  lifetimes (red line  $17\text{ s}^{-1}$ ; black line  $30\text{ s}^{-1}$ ; blue line  $54\text{ s}^{-1}$ ). The decay rate coefficients include the contribution of OH wall loss ( $1.4\text{ s}^{-1}$ ) in the flow tube, which needs to be subtracted to obtain atmospheric OH reactivities.

[Title Page](#)[Abstract](#)[Introduction](#)[Conclusions](#)[References](#)[Tables](#)[Figures](#)[I◀](#)[▶I](#)[◀](#)[▶](#)[Back](#)[Close](#)[Full Screen / Esc](#)[Printer-friendly Version](#)[Interactive Discussion](#)

OH reactivity  
measurement

S. Lou et al.

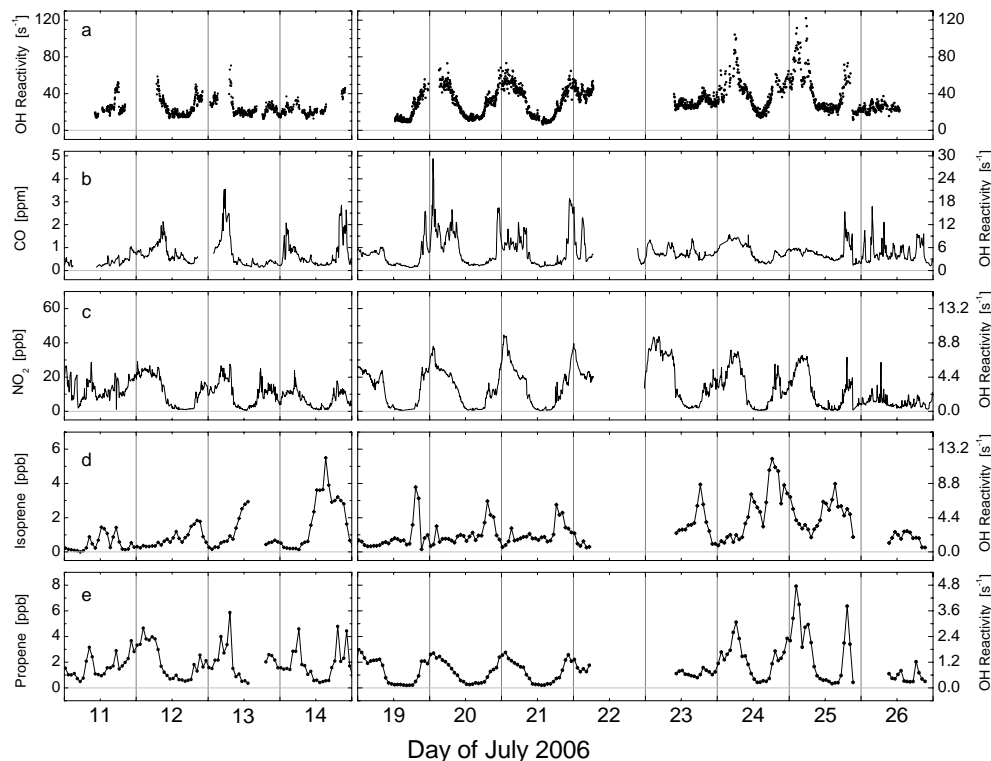


**Fig. 2.** Total OH reactivity (a) and volume mixing ratios of CO (b), NO<sub>2</sub> (c), isoprene (d) and propene (e) measured at Backgarden site in PRD from 11 to 27 July 2008. The right axis of panels (b)–(e) show corresponding reactivities of the individual trace gases. Data gaps at 15–18 and 22 July were caused by heavy rain during the typhoon BILIS and an electrical power blackout, respectively. Vertical lines denote midnight.

[Title Page](#)[Abstract](#)[Introduction](#)[Conclusions](#)[References](#)[Tables](#)[Figures](#)[◀](#)[▶](#)[◀](#)[▶](#)[Back](#)[Close](#)[Full Screen / Esc](#)[Printer-friendly Version](#)[Interactive Discussion](#)

OH reactivity  
measurement

S. Lou et al.

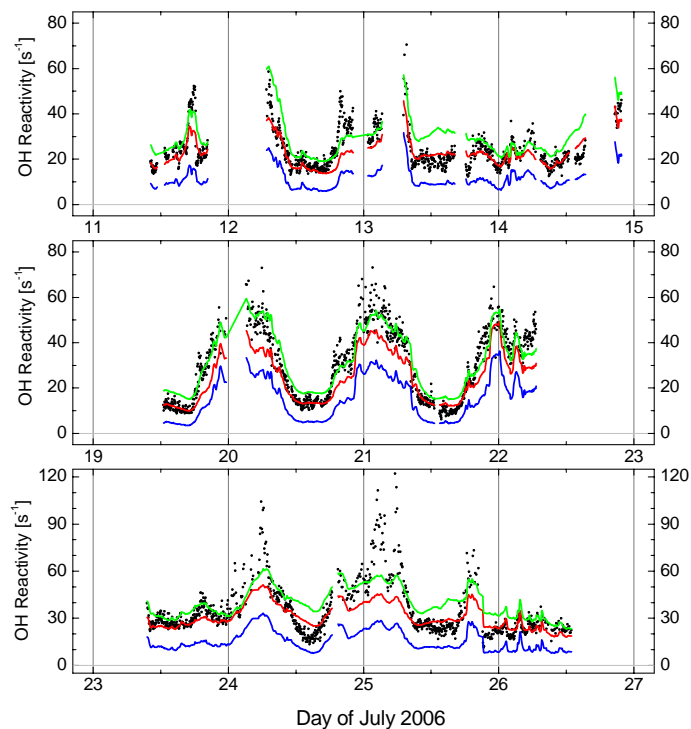


**Fig. 3.** Comparison of measured, calculated and modelled  $k_{\text{OH}}$  data at 1 atm and 313K. Dots: measured values. Blue line:  $k_{\text{OH}}^{\text{calc}}$  values calculated from measured trace gases (CO, NO<sub>x</sub>, hydrocarbons). Red line: model results,  $k_{\text{OH}}^{\text{model}}$  (RACM, base case). Green line: model results, using measured OH concentrations as an additional model constraint. Vertical lines denote midnight.

[Title Page](#)[Abstract](#)[Introduction](#)[Conclusions](#)[References](#)[Tables](#)[Figures](#)[◀](#)[▶](#)[◀](#)[▶](#)[Back](#)[Close](#)[Full Screen / Esc](#)[Printer-friendly Version](#)[Interactive Discussion](#)

OH reactivity  
measurement

S. Lou et al.

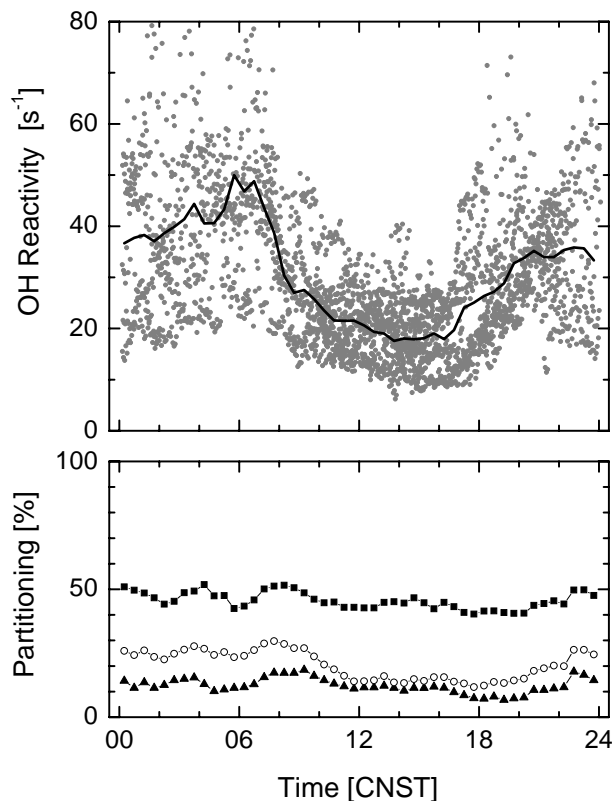


**Fig. 4.** Upper panel: diurnal variation of measured total OH reactivities at PRD for the days of 11–26 July 2006. Individual  $k_{OH}$  data are represented by gray dots and their half-hourly mean diurnal profile by the solid line. Lower panel: cumulative reactivities contributed by measured trace gases, normalized to the measured  $k_{OH}$ : CO (triangles), CO+NO<sub>x</sub> (open circles), CO+NO<sub>x</sub>+hydrocarbons (squares). The time of day is given in Chinese Standard Time (CNST=UTC+8 h), with solar noon at 12:30 CNST.

[Title Page](#)[Abstract](#)[Introduction](#)[Conclusions](#)[References](#)[Tables](#)[Figures](#)[◀](#)[▶](#)[◀](#)[▶](#)[Back](#)[Close](#)[Full Screen / Esc](#)[Printer-friendly Version](#)[Interactive Discussion](#)

OH reactivity  
measurement

S. Lou et al.

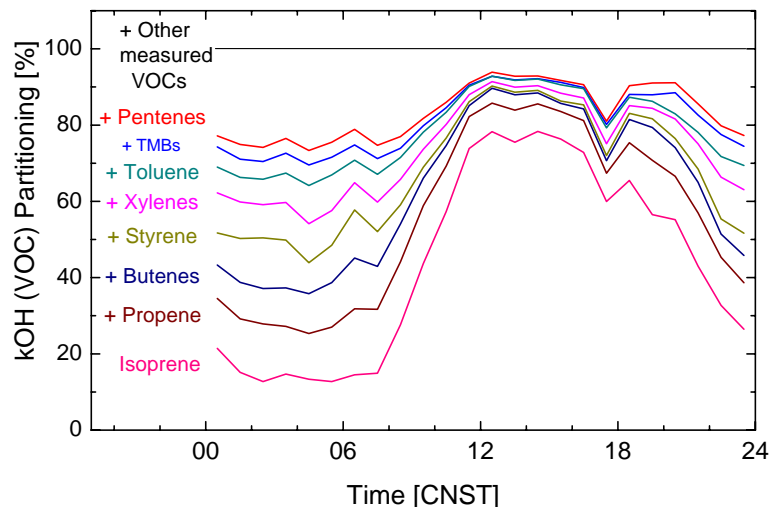


**Fig. 5.** Cumulative reactivities of measured hydrocarbons versus time of day, averaged for the days of 11–26 July 2006. The dominating VOC reactivities are displayed, normalized to the total reactivity of all measured hydrocarbons. The lowest (pink) line denotes isoprene, the next line (brown) denotes isoprene + propene, etc. Note: Butenes = 1-butene, *cis*-2-butene, *trans*-2-butene; pentenes = 1-pentene, *cis*-2-pentene, *trans*-2-pentene; xylenes = *o*-, *m*-, *p*-xylene; TMBs = 1,2,3-, 1,2,4-, 1,3,5-trimethylbenzene.

[Title Page](#)[Abstract](#)[Introduction](#)[Conclusions](#)[References](#)[Tables](#)[Figures](#)[◀](#)[▶](#)[◀](#)[▶](#)[Back](#)[Close](#)[Full Screen / Esc](#)[Printer-friendly Version](#)[Interactive Discussion](#)

OH reactivity  
measurement

S. Lou et al.

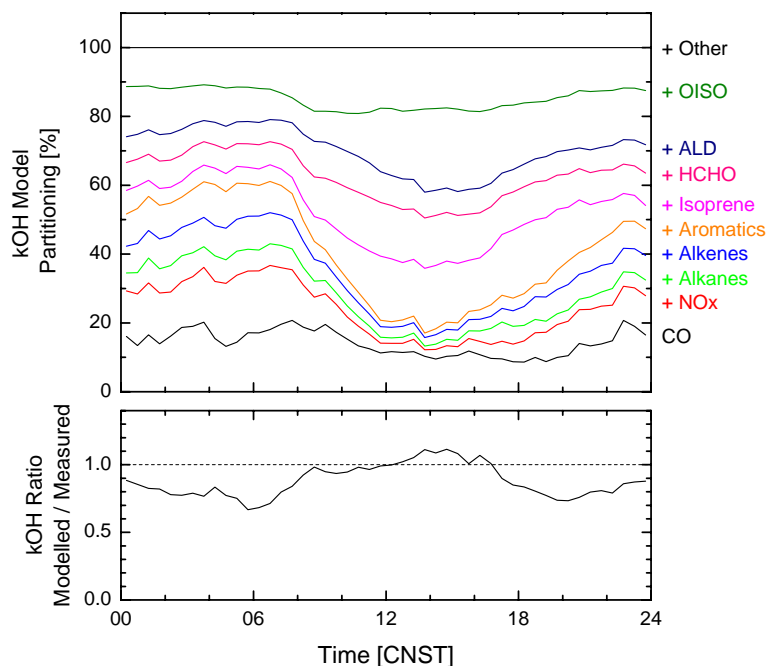


**Fig. 6.** Upper panel: cumulative OH reactivities of measured and modelled compounds normalized to the modelled, total OH reactivity. The data have been averaged for the days of 11–26 July 2006. Note: CO, NO<sub>x</sub>, alkanes, alkenes, aromatics, and isoprene were used as model constraints (Table 2). HCHO, ALD, OISO and Other are products calculated by the RACM model (base case). “Alkanes” include H<sub>2</sub>, methane and C<sub>2</sub>–C<sub>12</sub> compounds; “alkenes” include C<sub>2</sub>–C<sub>5</sub> compounds; “ALD” is the group of modelled aldehydes; “OISO” is the group of modelled oxygenated isoprene products (methyl-vinyl ketone, methacrolein etc.); “Other” comprise all other model generated products like ketones, organic peroxides, nitrates, peroxy nitrates, dicarbonyl compounds, etc. Lower panel: ratio of the modelled to measured total OH reactivity.

[Title Page](#)[Abstract](#)[Introduction](#)[Conclusions](#)[References](#)[Tables](#)[Figures](#)[◀](#)[▶](#)[◀](#)[▶](#)[Back](#)[Close](#)[Full Screen / Esc](#)[Printer-friendly Version](#)[Interactive Discussion](#)

OH reactivity  
measurement

S. Lou et al.

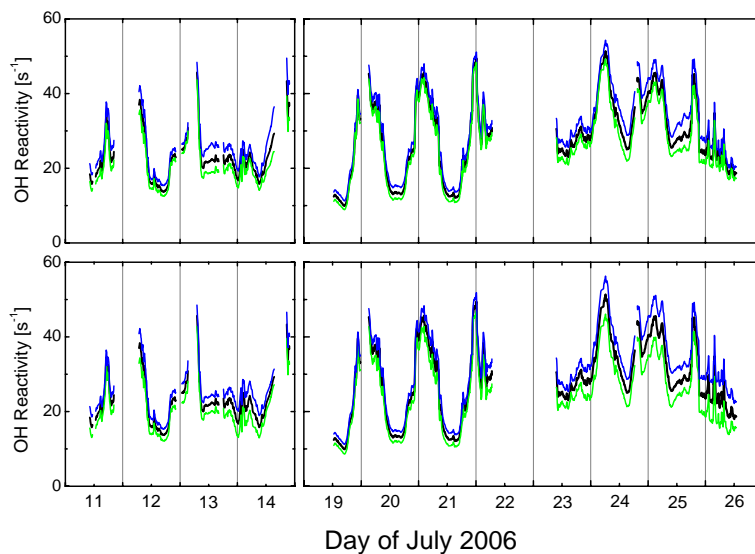


**Fig. 7.** Sensitivity test of modelled OH reactivities. Upper panel: variation of the OH concentration in the model runs. The black line represents the RACM model (base case) as shown in Fig. 3. The blue and green lines represent model results prescribing twice and half of the OH concentrations calculated in the base case run, respectively. Lower panel: variation of the deposition lifetime of modelled species. Black line: 24 h lifetime (base case); blue line: 48 h lifetime; green line: 12 h lifetime. Vertical lines denote midnight.

[Title Page](#)[Abstract](#)[Introduction](#)[Conclusions](#)[References](#)[Tables](#)[Figures](#)[◀](#)[▶](#)[◀](#)[▶](#)[Back](#)[Close](#)[Full Screen / Esc](#)[Printer-friendly Version](#)[Interactive Discussion](#)